

## NUMERICAL STUDY ON CHIRAL TURBULENCE OF ROTATING NEUTRINO MATTER IN SUPERNOVAE

**Hiomichi Kobayashi**

Department of Physics, Hiyoshi Campus  
Keio University  
4-1-1 Hiyoshi, Kohoku-ku Yokohama, Japan  
hkobayas@keio.jp

**Naoki Yamamoto**

Department of Physics  
Keio University  
3-14-1 Hiyoshi, Kohoku-ku, Yokohama, Japan  
nyama@rk.phys.keio.ac.jp

**Yoshihiro Okuno**

Department of Mechanical Engineering  
Tokyo Institute of Technology  
4259 Nagatsuta, Midori-ku, Yokohama, Japan  
okuno.y.aa@m.titech.ac.jp

### ABSTRACT

We numerically study the chiral turbulence of rotating neutrino matter in the core of supernovae. The rotation yields inverse cascade and the novel current along the direction of rotation called the chiral vortical effect. We for the first time demonstrate that the chiral vortical effect induces a flow in the direction of vorticity and a conversion from fluid helicity to neutrino density. These results may potentially lead to asymmetrical supernova explosions and the increase in the explosion energy in three-dimensional simulations.

### INTRODUCTION

After nuclear fusion reaction of a massive star having more than about 8 solar mass is completed, the core of the star contracts by the self-gravity and a core collapse occurs. It has been considered that the supernova explosion with a shock wave takes place by the bounce of the core collapse. In the core, electrons are captured by protons, and then neutrons and left-handed neutrinos are generated. The neutrinos carry away about 99% gravitational energy of the star toward the outside of the star.

The neutrino matter in the supernova core can be approximated as a fluid because the mean free path of neutrinos ( $\sim 1 \text{ cm} - 1 \text{ m}$ ) is short enough compared to the core size ( $\sim 100 \text{ km}$ ). However, Boltzmann equations are also used for the numerical simulation of the supernova explosion because hydrodynamic approximation of neutrino matter breaks down outside the core. A one-dimensional simulation for the neutrinos was conducted, and it was found that neutrino heating behind the shock wave is necessary (Kitaura et al., 2006). In a two-dimensional simulation, it became clear that the shock wave asymmetrically expands and blasts by a non-uniform energy concentration behind the shock wave (Marek and Janka, 2009). Nevertheless, in three-dimensional simulations, it has been difficult to reproduce explosions with the observed explosion energy. One of the reasons is that the energy cascade from large scales to small scales is dominant and the cascade deconcentrates the energy (Hanke et al., 2012; Takiwaki et al., 2014; Melson et al., 2015; Muller, 2015). For example, Takiwaki et al. (2014) reports that the three-dimensional simulations with high azimuthal angular resolutions reproduce only 15%~25% of the diagnostic explosion energy, while those with low azimuthal angular resolutions generate 35%~60% of the diagnostic explosion energy.

In previous studies, the feature that neutrinos have only left-handedness has not been considered. The property that mirror images do not coincide by parity transformation is termed as chirality. The chirality of a massless elementary particle is defined by the relative directions of spin and momentum, and the same direction is termed as right-handedness and the opposite direction is termed as left-handedness. In ordinal fluids, the fluid helicity is defined as the inner product of a velocity vector and a vorticity vector, and the chirality is characterized by the sign of the fluid helicity.

In relativistic matter of chiral elementary particles like neutrinos, there appears a novel current along the direction of vorticity, called the chiral vortical effect (CVE) (Vilenkin, 1979; Son and Surowka, 2009). Recently, Yamamoto (2016a, 2016b) found that the CVE of neutrinos drastically modifies the nonequilibrium hydrodynamic evolution of supernovae.

In the present study, we performed three-dimensional numerical simulations on the chiral turbulence of rotating neutrino matter in the core of the supernovae. We examined the influence of the rotation on inverse cascade, and we found that fluid helicity is converted to the neutrino density due to the CVE.

### BASIC EQUATIONS AND NUMERICAL METHODS

Three-dimensional turbulence obeying relativistic chiral hydrodynamics is examined under the system rotation around  $z$  axis. We set  $\hbar = c = e = 1$ . The momentum equations, the density equation and the equation of state with a thermodynamic relation (without the system rotation) are described as follows:

$$(\partial_t + \mathbf{v} \cdot \nabla) \mathbf{v} = -(\nabla p) / (\epsilon + p) + \nu \nabla^2 \mathbf{v} \quad (1)$$

$$\partial_t (n + \xi \mathbf{v} \cdot \boldsymbol{\omega}) + \nabla \cdot \mathbf{j} = 0, \quad \mathbf{j} = n \mathbf{v} + \xi \boldsymbol{\omega} \quad (2)$$

$$\epsilon + p = \mu n, \quad \epsilon = 3p = \mu^4 / 8\pi^2, \quad \xi = -\mu^2 / 24\pi^2 \quad (3)$$

where  $\mathbf{v}$  is the velocity,  $p$  is the pressure,  $\epsilon$  is the energy,  $\nu$  is the kinematic viscosity,  $n$  is the neutrino density,  $\boldsymbol{\omega}$  is the vorticity,  $\mu$  is the chemical potential and negative  $\xi$  denotes the transport coefficient of the CVE for left-handed neutrinos. In the presence of the system rotation, the Coriolis force is added in Eq. (1) and  $\boldsymbol{\omega}$  is replaced by  $\boldsymbol{\omega} + 2\boldsymbol{\Omega}$  in Eq. (2), where  $\boldsymbol{\Omega}$  is the angular velocity of the system rotation.

The finite difference method with the forth-order accuracy is adopted for the spatial discretization. The third-order Adams-

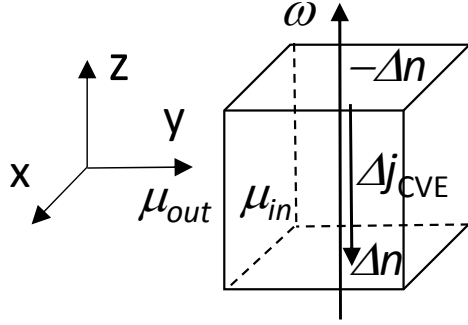


Figure 1. Generation of neutrino current in the direction of  $\omega$ .

Bashforth method is used for the time integration. The periodic boundary condition is adopted in  $x$ ,  $y$  and  $z$  directions.

The non-dimensional computational domain is  $2\pi \times 2\pi \times 2\pi$ . The grid points of  $128^3$  are used. We examined  $\Omega=0, 2$  and  $\pm 4$ . The time step is set to  $1.0 \times 10^{-2}$  and the time step number is  $1.0 \times 10^5$ . Initial velocities are composed of turbulence energy with spectra of  $k^{-5/3}$  for  $k > 16$  and  $k^{22}$  for  $k < 16$ , and the initial maximum velocity is 0.8. The initial distribution of the energy  $\epsilon$  is set to  $1+0.1v_x$ . An external random force is imposed at a wave number  $k=16$  to obtain the steady turbulence at  $\Omega=0$ . For  $\Omega=\pm 4$ , the external force is 1.6 times stronger than that for the others, because the energy spectra in high wave numbers decrease and laminarize.

In order to explain the consequences of the CVE, the schematic view of the generation of the neutrino current in the direction of  $\omega$  is shown in Fig. 1. If there is a difference of the chemical potential between the inside and outside of some finite domain as  $\mu_{in} - \mu_{out} > 0$ , a neutrino current  $\partial_z(\xi\omega) \approx -\mu/12\pi^2 \partial_z\mu\omega$  is generated by the CVE in Eq. (2). Thus, neutrino density becomes higher in the lower plane than in the upper plane. The high neutrino density leads to high pressure and energy in the lower plane from Eq. (3). The pressure gradient induces the vertical velocity in the direction of  $\omega$ . If there is no parity violation by the chirality of neutrinos, namely,  $\xi = 0$ , the neutrino density is conserved by  $\partial_t n = 0$  with the integration of the overall domain. However, if there are parity-violating effects, only the summation  $n + \xi \mathbf{v} \cdot \boldsymbol{\omega}$  is conserved. This means that, if the averaged vertical velocity contributes to the reduction of helicity  $\xi \mathbf{v} \cdot \boldsymbol{\omega}$ , the neutrino density  $n$  can increase. This is a new prediction for the increase the neutrino density (energy) due to the CVE.

## RESULTS AND DISCUSSION

Figure 2 shows time evolutions of energy and density spectra at  $\Omega=4$ . The initial distribution as shown by dashed line immediately changes to the line at  $t=10$ , and then inverse cascade is observed in energy and density spectra, respectively. The inverse cascade is caused by the strong rotation. If there is no rotation, inverse cascade is not observed. Figure 3 shows the energy and density spectra at  $t=1000$  for  $\Omega=0, 2$  and  $4$ . The condition of  $\Omega=2$  gives lower wave number peaks than that of  $\Omega=4$ . This means that the strong rotation suppresses the turbulence energy of high wave number and inverse cascade becomes slow. It is confirmed that an optimal angular velocity exists for a fast inverse cascade.

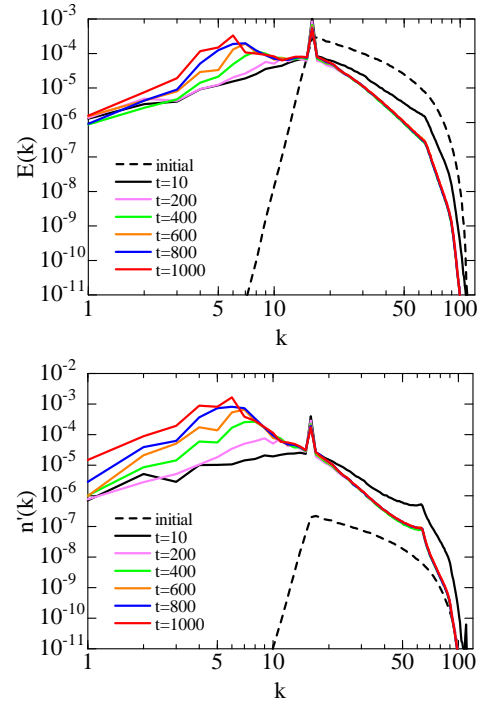


Figure 2. Time evolutions of energy and density spectra at  $\Omega=4$ .

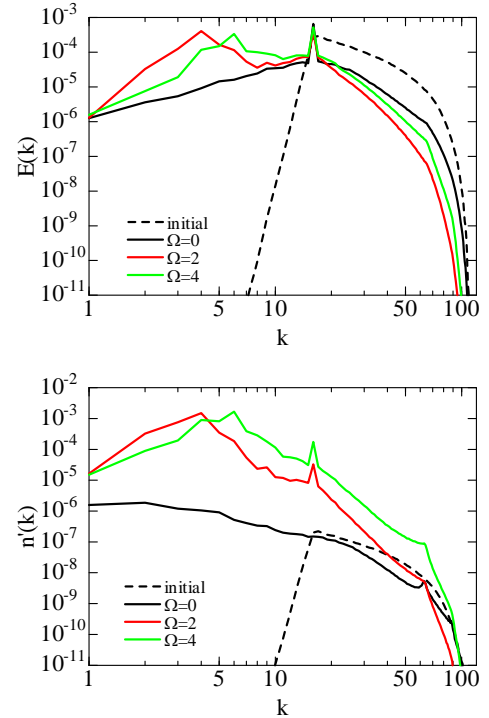


Figure 3. Energy and density spectra at  $t=1000$  for  $\Omega=0, 2$  and  $4$ .

Iso-surfaces of vorticity ( $\omega=3$ ,  $\omega_z > 0$  blue,  $\omega_z < 0$  red) and density ( $n=0.4$  yellow and  $0.5$  blue) at  $t=1000$  are visualized in Figs. 4 and 5. Although the direction of vorticity structures

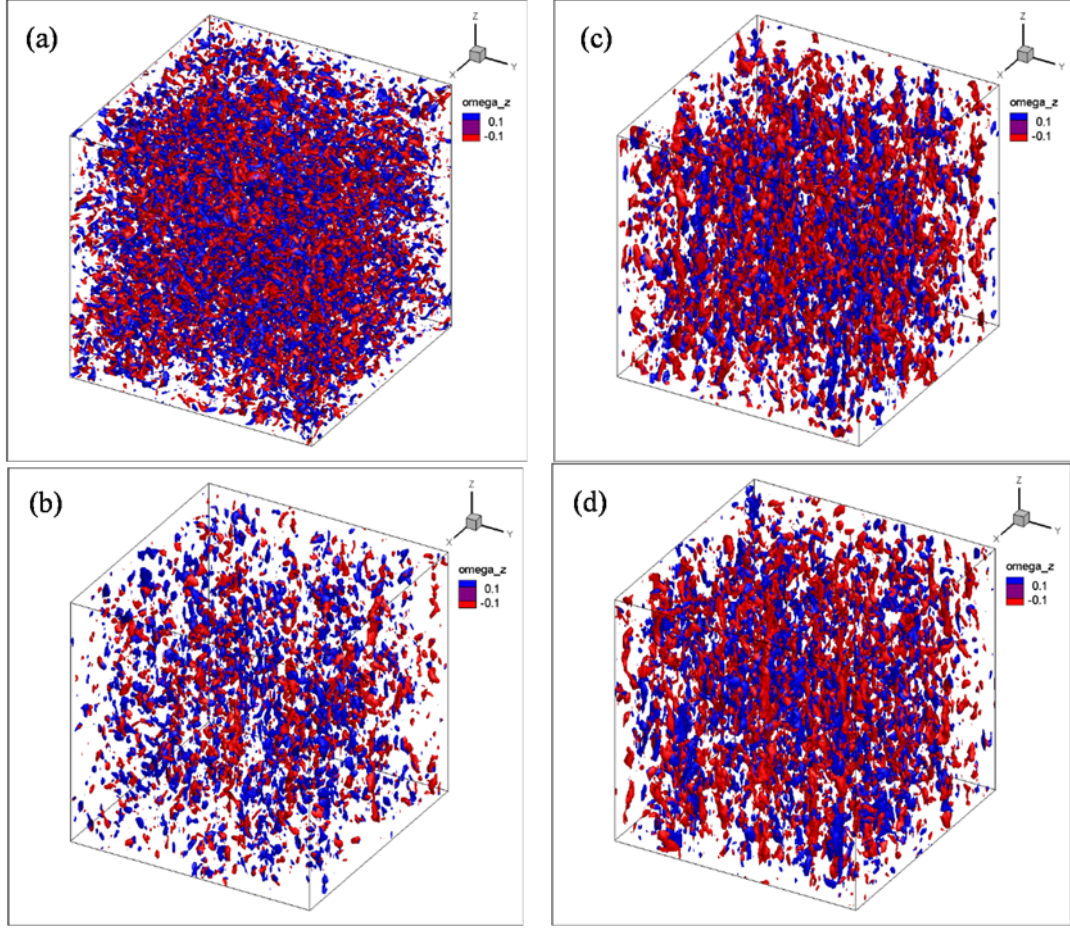


Figure 4. Iso-surfaces of vorticity ( $\omega=3$ ,  $\omega_z > 0$  blue,  $\omega_z < 0$  red) at  $t=1000$  for (a)  $\Omega=0$ , (b)  $\Omega=2$ , (c)  $\Omega=4$  and (d)  $\Omega=4$  without the chiral effect.

randomly distributes at  $\Omega=0$ , the vorticity structures are stretched in the  $z$  direction for  $\Omega=2$  and 4. The fine structures with positive and negative  $\omega_z$  align in the  $z$  direction for  $\Omega=2$  and 4. As seen in Fig. 3, the condition of  $\Omega=2$  effectively curbs the fine scale structures in Fig. 4(b). Iso-surfaces of density also align in the  $z$  direction and have relatively large structures like pillars for  $\Omega=2$  and 4. However, such pillar structures do not appear at  $\Omega=0$ . The system rotation causes inverse cascade and the quasi two-dimensional structures. It is considered that the density concentration aligned in the  $z$  direction leads to asymmetrical supernova explosions. It should be noted that the CVE seldomly affect the vortical structures as seen in Figs. 4(d) and 5(d).

Figure 6 depicts the density distribution and contour lines of turbulence energy in the  $x$ - $y$  plane at  $t=1000$  for  $\Omega=2$  and 4. It can be seen that the energy concentration emerges in the region of high density. The probability density function of the neutrino density concentrates 0.45 at  $\Omega=0$ , while at  $\Omega=4$  the maximum of the pdf moves to 0.41 and the pdf becomes broad (not shown here). It is found that the strong turbulence intensity concentrates in the high-density region. This is also a preferable feature for the asymmetrical supernova explosion.

Time evolutions of averaged pressure gradient, vertical velocity, density and helicity are shown in Fig. 7. As shown in

Fig. 1, the number current in the direction of vorticity causes the pressure gradient  $-\partial_z p / (\epsilon + p)$ . The pressure gradient induces the vertical velocity. The induced vertical velocity is proportional to the magnitude of system rotation.  $\Omega > 0$  results in  $v_z > 0$ , and  $\Omega < 0$  leads to  $v_z < 0$ . These results yield  $\partial_t(\xi \cdot \boldsymbol{\omega}) < 0$ , and thus  $\partial_t n > 0$  from Eq. (2). These phenomena are the nontrivial consequences of the CVE. If there is no system rotation or no chiral term including  $\xi$  in Eq. (2), the vertical velocity is never induced and the average density never augments. The increase in the average density corresponds to the increase in the average energy  $\epsilon$ . This is the first demonstration of the generation of the neutrino density from fluid helicity by the CVE.

## CONCLUSION AND FUTURE WORK

We examined the chiral turbulence of rotating neutrino matter in the core of the supernova by three-dimensional numerical simulations. In this study, it is found that the rotation is necessary to realize the chiral vortical effect. Under the rotation, the velocity is induced in the direction of the rotation axis and the neutrino density (energy) is generated from fluid helicity. Inverse cascade leads to two-dimensional neutrino density concentration and it contributes to the asymmetrical supernova explosion. This may be a candidate to explain the

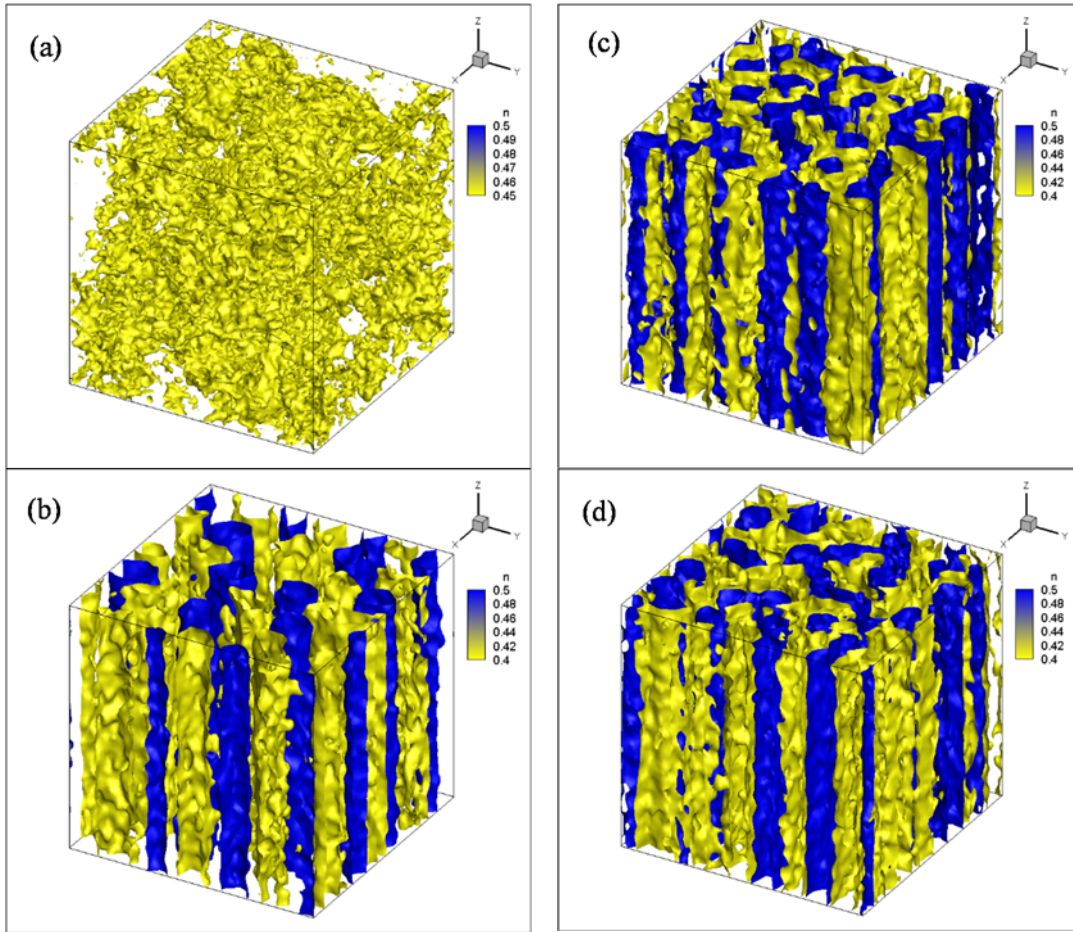


Figure 5. Iso-surfaces of neutrino density at  $t=1000$  for (a)  $\Omega=0$  ( $n=0.45$  yellow), (b)  $\Omega=2$ , (c)  $\Omega=4$  and (d)  $\Omega=4$  without the chiral effect ( $n=0.4$  yellow and  $0.5$  blue).

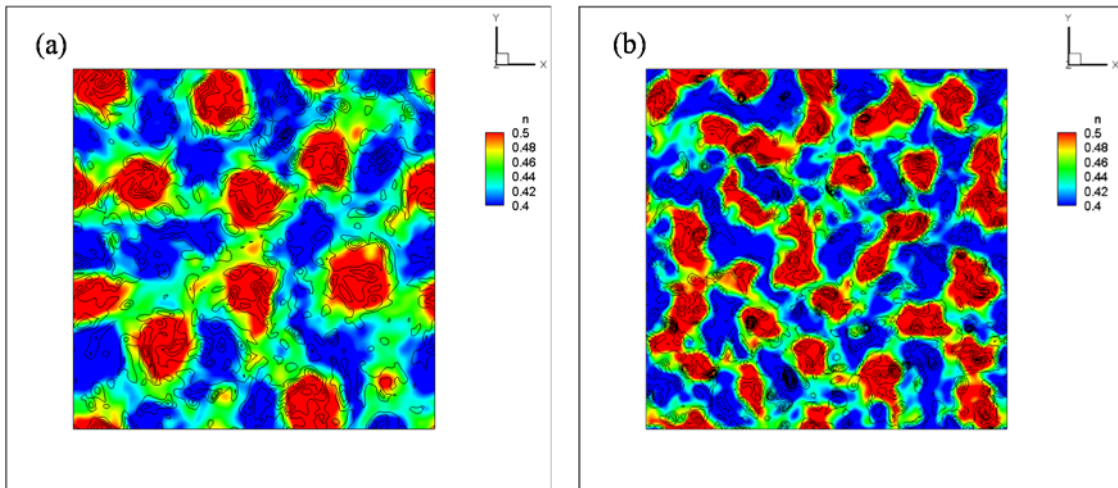


Figure 6. Density distribution and contour lines of turbulence energy in the  $x$ - $y$  plane at  $t=1000$  for (a)  $\Omega=2$  and (b)  $\Omega=4$ .

missing explosion energy of the supernova explosion when compared to the observed explosion energy.

**REFERENCES**

Hanke, F., Marek, A., Muller, B., Janka, H.-T., 2012, "Is Strong SASI Activity the Key to Successful Neutrino-Driven Supernova Explosions?", *Astrophys. J.*, Vol. 755, 138.

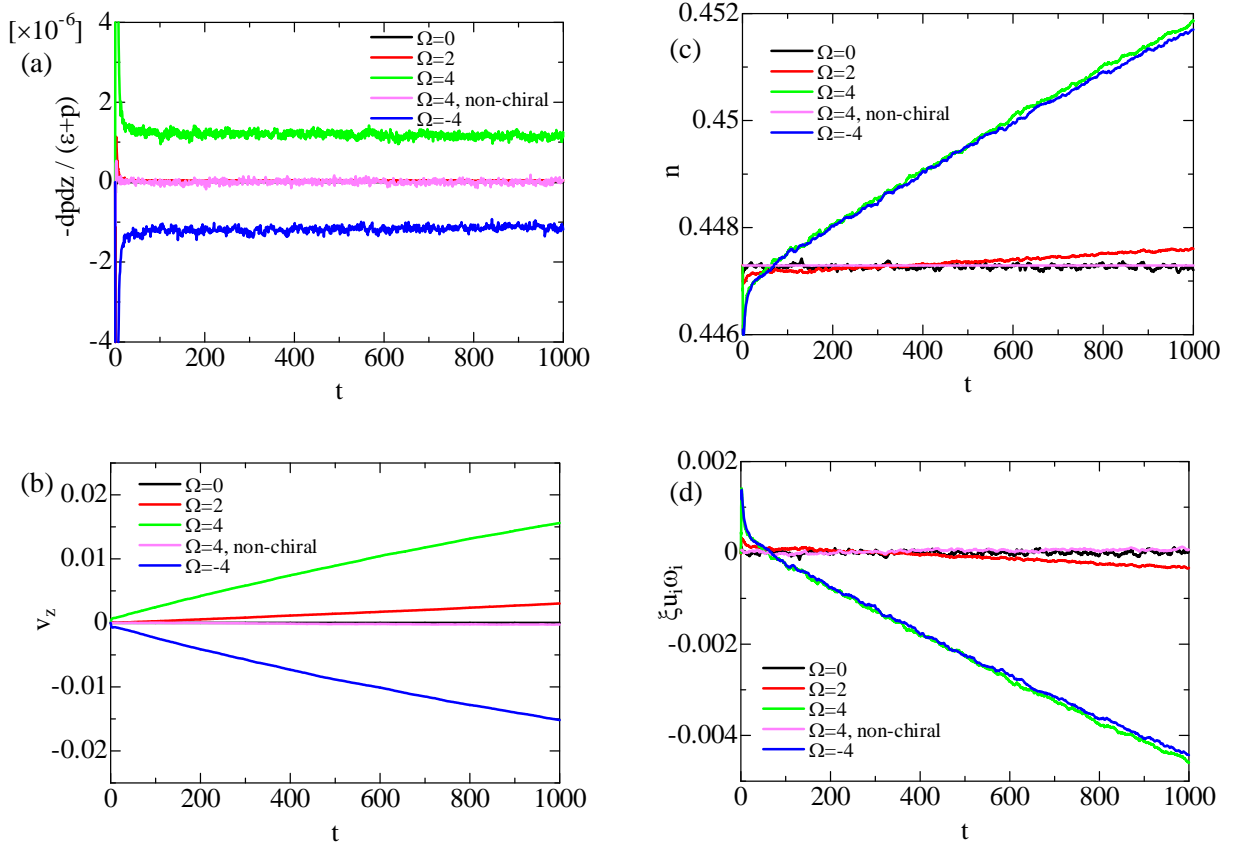


Figure 7. Time evolutions of (a) pressure gradient, (b) vertical velocity, (c) neutrino density and (d) helicity.

Kitaura, F. S., Janka, H.-T., Hillebrandt, W., 2006, “Explosions of O-Ne-Mg Cores, the Crab Supernova, and Subluminous Type II-P Supernovae”, *Astro. Astrophys.*, Vol. 450, pp. 345-350.

Marek, A., Janka, H.-T., 2009, “Delayed Neutrino-Driven Supernova Explosions Aided by the Standing Accretion-Shock Instability”, *Astrophys. J.*, Vol. 694, pp. 664-696.

Melson, T., Janka, H.-T., Marek, A., 2015, “Neutrino-Driven Supernova of a Low-Mass Iron-Core Progenitor Boosted by three-Dimensional Turbulent Convection”, *Astrophys. J. Lett.*, Vol. 801, L24.

Muller, B., 2015, “The Dynamics of Neutrino-Driven Supernova Explosions after Shock Revival in 2D and 3D”, *Mon. Not. Roy. Astron. Soc.*, Vol. 453, pp. 287-310.

Son, D. T., Surowka, P., 2009, “Hydrodynamics with Triangle Anomalies”, *Phys. Rev. Lett.*, Vol. 103, 191601.

Takiwaki, T., Kotake, K., Suwa, Y., 2014, “Comparison of Two- and Three-Dimensional Neutrino-Hydrodynamics Simulations of Core-Collapse Supernovae”, *Astrophys. J.*, Vol. 86, 83.

Vilenkin, A., 1979, “Macroscopic Parity-Violating Effects: Neutrino Fluxes from Rotating Black Holes and in Rotating Thermal Radiation”, *Phys. Rev. D*, Vol. 20, pp. 1807-1812.

Yamamoto, N., 2016a, “Chiral Transport of Neutrinos in Supernovae: Neutrino-Induced Fluid Helicity and Helical Plasma Instability”, *Phys. Rev. D*, Vol. 93, 065017.

Yamamoto, N., 2016b, “Scaling Laws in Chiral Hydrodynamic Turbulence”, *Phys. Rev. D*, Vol. 93, 125016.